

Observation of a Novel Electron Paramagnetic Resonance in Germanium Containing Dislocations

E. J. Pakulis and C. D. Jeffries

Materials and Molecular Research Division, Lawrence Berkeley Laboratory, and Department of Physics, University of California, Berkeley, California 94720

(Received 25 September 1981)

The first observation of EPR of electrons at dislocations in Ge is reported. Under optical excitation two sets of lines are detected: four lines about the $\langle 111 \rangle$ axes with $g_{\parallel} = 0.34$ and $g_{\perp} = 1.94$, and 24 lines with $g_{\parallel} = 0.73$ and $g_{\perp} = 1.89$ about $\langle 111 \rangle$ axes with a six-fold 1.2° distortion. The lines persist for hours after excitation and are inverted in sign.

PACS numbers: 76.30.Mi, 61.70.Le, 71.55.Fr, 72.20.Jv

In contrast to the case of Si, reports of EPR in Ge have been few, restricted to group-V donor atoms¹⁻³ and the Li-O complex.⁴ We report here two new sets of EPR lines⁵ in optically excited dislocated *n*-type Ge at liquid He temperatures. We associate these highly anisotropic lines with electrons at dislocations. The lines appear after optical excitation and persist for hours, indicating an extraordinarily long-lived excited state, as in Si (Ref. 6); they have opposite sign from normal EPR absorption of donors. In fact, we believe that the negative absorption is actually due to a decrease in sample conductivity detected by the cavity electric field rather than to the usual EPR magnetic dipole absorption.⁷

The apparatus used was a He-cooled microwave (22–26 GHz) superheterodyne spectrometer with an optical port and a He-cooled shutter. Magnetic field modulation and lock-in detection were used to record the derivative of the absorption signal. Samples were cut from nine different Czochralski-grown Ge single crystals supplied by W. L. Hansen and E. E. Haller. The crystals were *n* type, with a net donor (As and/or P) concentration ranging from 5×10^9 to 8×10^{13} cm⁻³, and dislocation etch-pit densities between 10^3 and 10^5 cm⁻². None of the new lines were observed in a dislocation-free crystal. A typical sample was cut in the shape of a right circular cylinder, 12.5×10 mm², polished, etched, mounted in the spectrometer cavity, and cooled to liquid He temperatures, with the optical shutter closed. At $T \lesssim 4$ K the Ge sample itself becomes a microwave resonant dielectric cavity with a large quality factor, $Q \gtrsim 10^5$.⁸ This makes the present experiment possible, with signal/noise $\sim 30:1$. Two modes of excitation were used: (1) broadband light from a Hg-vapor arc lamp, which produced EPR signals after but not during excitation; and (2) arc lamp through a 2-mm-thick RT Ge filter which together with Dewar windows limited the

excitation to sub-band-gap energies $0.3 < E < 0.7$ eV, and produced EPR lines both during and after pumping. In all cases the lines are undetectable before shutter opening, and persist for at least 4 h after closing.

Two new sets of lines are observed: 24 narrow lines (14-G peak-to-peak derivative width), and four broad lines (40 G peak to peak). When the magnetic field is along a $\langle 100 \rangle$ axis, all 28 lines converge to the simple spectrum centered at $g \cong 1.6$ shown in Fig. 1, adjacent to the As donor hyperfine structure. Crystals grown in a hydrogen atmosphere gave lines reversed in sign with respect to the shallow-donor hyperfine structure. Those grown in argon or vacuum gave nonreversed lines.

When the magnetic field was rotated approximately in the (110) plane, we observed the complex spectrum of the narrow lines shown in Fig. 2. It consists of four main branches: two with six resolved lines each, and two branches which appear to have only three lines but actually become resolved into six when the magnetic field

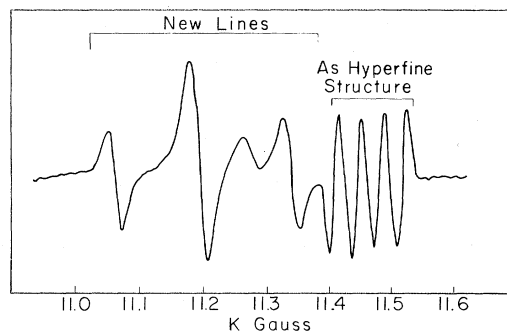


FIG. 1. Derivative curves of EPR in As-doped Ge ($N_D - N_A = 8 \times 10^{13}$ cm⁻³). Magnetic field is oriented along a $\langle 100 \rangle$ direction. $T = 2$ K, $f = 25.16$ GHz. Note the sign reversal of the new lines as compared to the As hyperfine structure. Dislocation density $\approx 2 \times 10^4$ cm⁻².

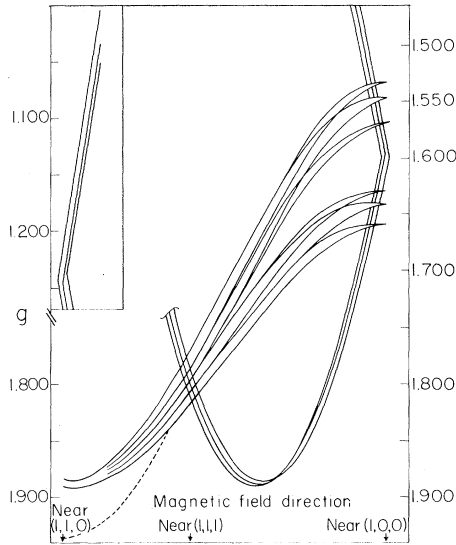


FIG. 2. Angular dependence of the \bar{g} tensor for the narrow new lines in a sample of P-doped Ge ($N_D - N_A = 10^{12} \text{ cm}^{-3}$) as the magnetic field is rotated in a plane tilted $\sim 3^\circ$ from a $\langle 110 \rangle$ plane. Inset shows the continuation of the lines for low values of g near $\langle 110 \rangle$. No data were taken for $g < 1$, corresponding to $H > 19 \text{ kG}$, the limit of the magnet used. $T = 2 \text{ K}$, $f = 26.06 \text{ GHz}$, dislocation density $\approx 1 \times 10^4 \text{ cm}^{-2}$. The dashed line shows a portion of one of the four broad lines.

is rotated in a different plane. The overall symmetry of the four branches is that of the four $\langle 111 \rangle$ axes, so each $\langle 111 \rangle$ axis contributes six narrow lines. Had the magnetic field been exactly in the $\langle 110 \rangle$ plane, the two branches with six resolved lines each would have become superposed. The line intensity from one of the $\langle 111 \rangle$ axes is typically five to ten times that of the others; this behavior is explicable for a distribution of spins on line defects, but not point defects. Figure 2 also shows, for comparison, one of the broad lines (dashed); they have no resolved structure and have symmetry axes along the $\langle 111 \rangle$ directions.

The observed EPR spectra can be described by the effective spin Hamiltonian $\mathcal{H} = \mu_B \vec{H} \cdot \bar{g} \cdot \vec{S}$, where μ_B is the Bohr magneton, \vec{H} the magnetic field, \bar{g} the spectroscopic tensor, and \vec{S} the spin. For the four broad lines, $S = \frac{1}{2}$ and \bar{g} is axially symmetric about the four $\langle 111 \rangle$ axes with

$$g_{\parallel} = 0.336 \pm 0.005; \quad g_{\perp} = 1.939 \pm 0.005. \quad (1)$$

For the 24 narrow lines, $S = \frac{1}{2}$ and \bar{g} is axially symmetric about the 24 directions

$$\langle 111 \rangle_i \pm \alpha \langle 110 \rangle_j, \quad i = 1 \text{ to } 4, \quad j = 1 \text{ to } 6, \quad (2)$$

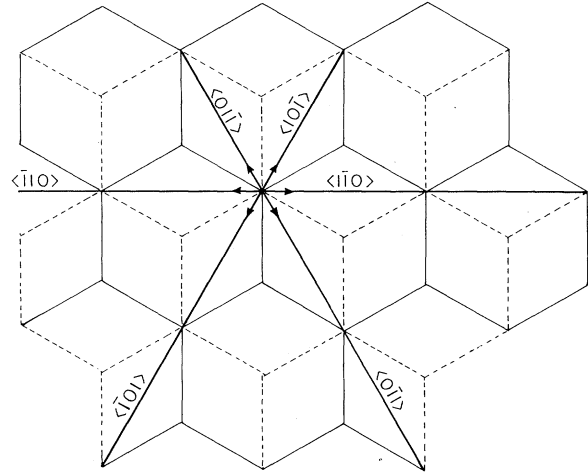


FIG. 3. Projection of the Ge crystal structure onto the $\langle 111 \rangle$ plane. The heavy labeled lines are the $\langle 110 \rangle$ axes in that plane. The six arrows, not to scale, are projections of six of the symmetry directions of the \bar{g} tensor for the narrow new lines.

such that $\langle 111 \rangle_i \cdot \langle 110 \rangle_j = 0$. The parameter α is a measure of the deviation, along a $\langle 110 \rangle$ direction, of each symmetry direction away from a given $\langle 111 \rangle$ axis. The data yield $\alpha = 0.02$, which corresponds to a 1.2° distortion. The principal g values for the narrow lines are

$$g_{\parallel} = 0.730 \pm 0.005; \quad g_{\perp} = 1.889 \pm 0.005. \quad (3)$$

In Fig. 3 we illustrate the six EPR symmetry directions associated with a particular $[111]$ axis. Since dislocation lines run along $\langle 110 \rangle$ directions,⁹ we see that a symmetry axis is tilted along a dislocation line perpendicular to the $[111]$ axis. If the EPR signal is due to dislocation dangling bonds (DDB), then the \bar{g} -tensor symmetry axis will be along the direction of the DDB. Our results indicate that the type of dislocation responsible is one in which the DDB are nearly perpendicular to the dislocation line. The familiar 60° dislocation of the shuffle set, Fig. 4, is of this variety.¹⁰

The 1.2° tilt of the DDB could be an intrinsic distortion characteristic of the dislocation or it could be the result of a Peierls-like instability. In the case of intrinsic distortion, there are several geometries which are consistent with the data: (1) All DDB in a given dislocation are tilted in the same direction, and along the dislocation line. (2) The DDB are tilted alternately in opposite directions along the dislocation line. (3) The DDB are tilted in the direction of the

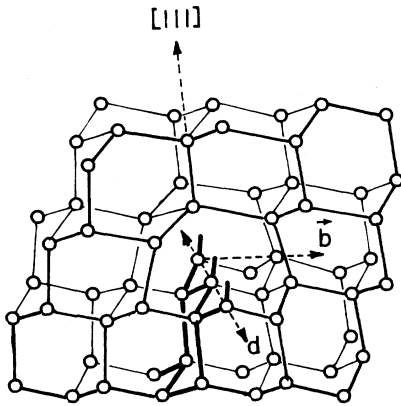


FIG. 4. Ge crystal structure including one 60° dislocation line, d , with its row of DDB, and Burgers vector \vec{b} . See Ref. 10.

Burgers vector. In principle, one could test for this possibility by selectively inducing dislocations in one direction and then observing the tilt direction in the EPR \vec{g} -tensor axis.

Alternatively, the distortion may be the result of an instability with respect to dimerization of a linear chain of charges and/or spins. For example, Pincus¹¹ has demonstrated the spontaneous distortion of a uniform antiferromagnetic chain into an alternating antiferromagnet. Evidence of such a spin-Peierls transition has been observed¹² in some physical systems.

For normal EPR magnetic dipole absorption lines, as detected by the magnetic field of the cavity, sign reversal could result from spin population inversion created by spin-dependent relaxation processes in the optical pumping cycle. In our case, however, this interpretation cannot explain the persistence of the lines for hours after removal of optical pumping and after repeated passage through spin resonance. It is also difficult to account for the size of the signal, given the small number of DDB in the samples.

The signal reversal can instead be explained as a decrease in the conductivity of the crystal as sampled by the cavity electric field, but under microwave spin resonance conditions. The drop in conductivity due to spin flips appears as an increase in cavity Q , and hence a reversed signal. A conductivity decrease on passage through spin resonance has been observed by Grazhulis, Kveder, and Osip'yan¹³ in He-cooled dislocated Si under constant illumination. They interpreted the spin-dependent photoconductivity as a spin-dependent scattering of free carriers by dislocations. Wosinski, Figielski, and Makosa⁷ also

observed spin-dependent photoconductivity in dislocated Si under steady illumination and showed that it gave rise to a reversed EPR signal; they explain this through spin-dependent recombination of free carriers. In our experiments on Ge, however, we observe the reversed EPR lines even after the light has been switched off and long after the decay of all free carriers. We propose that, in Ge, photoexcited electrons can become trapped for hours in a dislocation band with a nonzero conductivity which depends on their spin orientation relative to spins at DDB. Conductivity changes would occur each time either the excited electrons or the DDB electrons undergo spin flips. Presumably their \vec{g} tensors would not be the same, i.e., the four broad lines may be those of the excited electrons, the 24 narrow lines those of the DDB electrons. The difference in sign between a hydrogen-grown crystal (Q increases) and a vacuum-grown crystal (Q decreases) is very likely due to the presence of hydrogen at dislocations.¹⁴ Spin-dependent *increases* in conductivity have been observed by Szkielko¹⁵ in dislocated Si *p-n* junctions. He attributed his results to spin-dependent generation of carriers at dislocations.

In summary, using the ultrasensitive technique of high- Q self-resonant samples and electric detection of magnetic resonance, we have been able to study Ge crystals of low dislocation densities. A wealth of new electric detection of magnetic resonance lines emerged which through their symmetry yield evidence of a small well-defined distortion within dislocations. At the same time, their sign reversal and excitation-decay properties indicate the possibility of a long-lived dislocation conduction band with spin-dependent mobility.

We would like to thank W. L. Hansen and E. E. Haller for providing the Ge crystals, and J. W. Bray, E. E. Haller, A. M. Portis, and L. M. Falicov for helpful discussions. This work was supported by the Director, Office of Energy Research, Office of Basic Energy Sciences, Material Sciences Division of the U. S. Department of Energy under Contract No. W-7405-ENG-48.

¹G. Feher, D. K. Wilson, and E. Gere, *Phys. Rev. Lett.* **3**, 25 (1959).

²D. K. Wilson, *Phys. Rev.* **134**, A265 (1964).

³R. E. Pontinen and T. M. Sanders, Jr., *Phys. Rev.*

152, 850 (1966).

⁴E. E. Haller and L. M. Falicov, Phys. Rev. Lett. 41, 1192 (1978).

⁵E. J. Pakulis and C. D. Jeffries, Bull. Am. Phys. Soc. 26, 223 (1981).

⁶E. Weber and H. Alexander, J. Phys. (Paris), Colloq. 40, C6-101 (1979).

⁷T. Wosinski, T. Figielski, and A. Makosa, Phys. Status Solidi (a) 37, K57 (1976).

⁸For a detailed analysis of a high- Q microwave resonant sample, see A. Okaya and L. F. Barash, Proc. IRE 50, 2081 (1962). Our apparatus was designed for high- Q TiO₂ resonant samples; its first use with high- Q resonant germanium samples was by Haller and Falicov (Ref. 4) and E. E. Haller, W. L. Hansen, and

F. S. Goulding, Adv. Phys. 30, 93 (1981), who found large signal enhancements.

⁹See, e.g., H. Alexander and P. Haasen, in *Solid State Physics: Advances in Research and Applications*, edited by Frederick Seitz, David Turnbull, and Henry Ehrenreich (Academic, New York, 1968), Vol. 22, p. 27.

¹⁰J. Hornstra, J. Phys. Chem. Solids 5, 129 (1958).

¹¹P. Pincus, Solid State Commun. 9, 1971 (1971).

¹²I. S. Jacobs *et al.*, Phys. Rev. B 14, 3036 (1976).

¹³V. A. Grazhulis, V. V. Kveder, and Yu. A. Osip'yan, Pis'ma Zh. Eksp. Teor. Fiz. 21, 708 (1975) [JETP Lett. 21, 335 (1975)].

¹⁴Haller, Hansen, and Goulding, Ref. 8.

¹⁵W. Szkielko, Phys. Status Solidi (b) 90, K81 (1978).

ERRATA

NONSTATIC SPIN-ISOSPIN ORDER IN LIGHT NUCLEI. N. Lo Iudice and F. Palumbo [Phys. Rev. Lett. 46, 1054 (1981)].

We have used Weisskopf units for the $B(M2)$ in Table I without distinction between absorption and decay. The conversion factor $1 \text{ W.u.} = 15.2 \mu_N^2 \text{ fm}^2$ should therefore be used. It would have been more appropriate to use Weisskopf units for absorption, which are five times larger.

MEASUREMENT OF THE ANGULAR DISTRIBUTION OF TENSOR POLARIZATION IN PION-DEUTERON ELASTIC SCATTERING. R. J. Holt, J. R. Specht, K. Stephenson, B. Zeidman, J. S. Frank, M. J. Leitch, J. D. Moses, E. J. Stephenson, and R. M. Laszewski [Phys. Rev. Lett. 47, 472 (1981)].

Square-root signs were inadvertently omitted from the expression for t_{20} in the laboratory frame. The correct expression is

$$t_{20}^{\text{lab}} = \frac{1}{2} t_{20}^{\text{c.m.}} (3 \cos^2 \alpha - 1) + \left(\frac{3}{2}\right)^{1/2} t_{21}^{\text{c.m.}} \sin 2\alpha + \left(\frac{3}{2}\right)^{1/2} t_{22}^{\text{c.m.}} \sin^2 \alpha.$$

This correction does not affect any of the results presented.